Journal of Animal Ecology

British Ecological Society

Journal of Animal Ecology 2013, **82,** 572–586 doi: 10.1111/1365-2656.12027

Inferring spatial memory and spatiotemporal scaling from GPS data: comparing red deer *Cervus elaphus* movements with simulation models

Arild O. Gautestad[1], Leif E. Loe[2] and Atle Mysterud[1]*

[1]*Department of Biology, Centre for Ecological and Evolutionary Synthesis, University of Oslo, P.O. Box 1066 Blindern, Oslo, NO-0316, Norway; and* [2]*Department of Ecology and Natural Resource Management, Norwegian University of Life Sciences, P.O. Box 5003, Aas, NO-1432, Norway*

Summary

1. Increased inference regarding underlying behavioural mechanisms of animal movement can be achieved by comparing GPS data with statistical mechanical movement models such as random walk and Lévy walk with known underlying behaviour and statistical properties.

2. GPS data are typically collected with ≥ 1 h intervals not exactly tracking every mechanistic step along the movement path, so a statistical mechanical model approach rather than a mechanistic approach is appropriate. However, comparisons require a coherent framework involving both scaling and memory aspects of the underlying process. Thus, simulation models have recently been extended to include memory-guided returns to previously visited patches, that is, site fidelity.

3. We define four main classes of movement, differing in incorporation of memory and scaling (based on respective intervals of the statistical fractal dimension D and presence/absence of site fidelity). Using three statistical protocols to estimate D and site fidelity, we compare these main movement classes with patterns observed in GPS data from 52 females of red deer (*Cervus elaphus*).

4. The results show best compliance with a scale-free and memory-enhanced kind of space use; that is, a power law distribution of step lengths, a fractal distribution of the spatial scatter of fixes and site fidelity.

5. Our study thus demonstrates how inference regarding memory effects and a hierarchical pattern of space use can be derived from analysis of GPS data.

Key-words: fractal geometry, Lévy walk, memory map, multi-scaled random walk, site fidelity

Introduction

The mechanistic basis of individual movement is of key importance to the understanding of spatio-temporal dynamics of animal distribution (Getz & Saltz 2008; Nathan *et al.* 2008; Mueller, Fagan & Grimm 2011). For example, a change in the spatial distribution of grazing of a large herbivore after recovery of a large predator was a key to the understanding of trophic cascading effects on the entire ecosystem of Yellowstone, USA (Fortin *et al.* 2005). GPS data now provide very detailed information on animal movements, yet exploiting their full potential remain challenging (Morales *et al.* 2004). One way to derive further inference regarding underlying behavioural mechanisms is by comparing real movements with those from statistical mechanical movement models such as Brownian motion-like random walk (RW), correlated RW or Lévy walk (LW) (Bartumeus & Levin 2008; Sims *et al.* 2012). However, many of the theoretical models lack the necessary width of scope to fully exploit the potential to understand the underlying behavioural mechanisms of space use; for example, central place foragers or animals with other kinds of strong site fidelity. Inference can be gained by comparing models of increasingly higher level of realism in terms of simulated behaviour to the real data. We here provide such an attempt.

Behavioural ecologists reached a consensus a long time ago that mammals and many other taxonomic groups

*Correspondence author. E-mail: atle.mysterud@bio.uio.no

have the capacity to utilize spatially explicit information from the past, that is, a cognitive map, during relocation (Bailey 1995; Ostfeld & Manson 1996; Wolf *et al.* 2009). However, most mechanistic modelling of animal space use rests on a premise of short-term memory only, that is, a kind of behaviour where the next displacement is a function of near-term historic conditions and not dependent on the older history (termed 'Markovian'; Gautestad & Mysterud 2005; Viswanathan *et al.* 2011). Thus, the steps following direction-influencing events, such as an attraction towards or repellence from an object that appears within an individual's trailing perceptual field, will not be influenced by the direction or speed prior to the interrupt, that is, so-called memory-less locomotion (Gautestad & Mysterud 2005; Mueller, Fagan & Grimm 2011). Without long-term memory, any goal the animal may have been locked into becomes 'erased' by the new event and thus new events override the prior goal. Such movements influenced only by short-term memory may be optimal under conditions of relatively unpredictable distribution of resource patches (see Discussion: Context-specific site fidelity).

Many ecologists would argue for some kind of path analysis when analysing GPS data in detail. However, GPS data are typically collected with ≥ 1 h intervals or so, that is, they are not exactly tracking every mechanistic step along the movement path. The mechanistic scale is in this context the temporal resolution (observation interval) where the causality between environmental input, the animal's internal mode (e.g. hungry, scared or tired) and spatial displacement may be studied in detail. Thus, at a GPS sampling scale of 1 h a displacement between two successive relocations will typically reflect the sum of many intermediate decisions about where to move (or stay put). Hence, the path at this coarser resolution has to be described by a stochastic model design. This is a critical issue when comparing theoretical movement models with GPS data. Further, since directional persistence (path autocorrelation) is often found between successive relocations, despite a sampling interval of 1 h or more, stochastic movement models like RW have been refined by adding a higher level of persistence in direction (correlated RW). However, a correlated RW becomes a RW if you subsample larger than the minimum time interval when correlation in step length and direction disappears (Turchin 1996).

At mechanistic ('behavioural') time-scale, successive displacements are under the Markovian premise a function of the interplay between the individual's internal state and inputs from the environment within a narrow-range 'working memory' temporal scale. Consider high-frequency locations A→B→C→D→E→F→G→ … along a path, where the behavioural mechanisms ('movement rules', limited by working memory) may be deterministic, stochastic or a mixture. When an observer collects GPS fixes from this detailed path at a substantially larger time lag, the path at this coarser scale will appear Brownian motion like even if the behaviour at the mechanistic scale is deterministic: both the net displacement since last fix (observed step length) and the step direction becomes randomized, due to the intermediate sequence of independent movement-influencing events. In other words, if only steps between locations A→D→G are considered, the path is observed at time-scales where successive steps are characterized statistically like drawing direction and length independently from one step to the next. This difference in temporal scale separates mechanistic models (fine scale) and statistical mechanical models (coarse scale) (Fig. 1a).

The previous lack of explicit implementation of long-term memory effects on space use in theoretical movement models are now rapidly changing. In the 'Memory enhanced random walk' (MemRW) approach, mechanistic simulations have been extended with memory-dependent rules for return steps to previously visited patches (Dalziel, Morales & Fryxell 2008; Mueller & Fagan 2008; Van Moorter *et al.* 2009; Mueller, Fagan & Grimm 2011). Here, spatial memory is implemented to allow for an extension of the physical field of perception: distant aspects of the environment are successively considered (helped by memory) as a supplement to directly perceived neighbourhood information when the next step's direction is decided upon. This property is typically achieved in simulations by a direction-biased correlated RW to stimulate attraction towards known resource patches. Occasional return events to a previous location lead to the emergence of site fidelity. Operationally, MemRW is like a RW where the perceptual field (circles surrounding dots in Fig. 1a) is increased far beyond the physical range of the animal's senses, but where the movement rules are still executed in a mechanistic manner on the basis of local strength of the directional bias of step direction at the present point in time. Thus, a MemRW type of memory-influenced space use is satisfying the premise of a Markov process. The process is influenced by historic knowledge about distant local conditions, but this information is influencing movement in a spatially and temporally scale-specific manner (cfr. Gautestad & Mysterud 2010a). While previous simulations of movement under the statistical mechanical class MemRW have been studied at the mechanistic level, we are in the present context of analysis of GPS fixes focusing on the properties of MemRW at the statistical mechanical level (see Fig. 1a for a distinction between the 2 levels). For MemRW at the mechanistic level, habitat heterogeneity is explicitly modelled, while at the statistical mechanical level, this complexity may be transformed and simplified into specific model parameters and other properties that characterize this movement class.

The Brownian motion/random walk paradigm (RW) has also been challenged with respect to whether animals under specific conditions tend to perform LW-like displacements with a 'fat' power law tail in the step length distribution, that is, the frequency of very long exploratory steps are more probable than for a Brownian motion or correlated RW (Hagen *et al.* 2001; Sims *et al.* 2008; Humphries *et al.* 2010; Viswanathan *et al.* 2011).

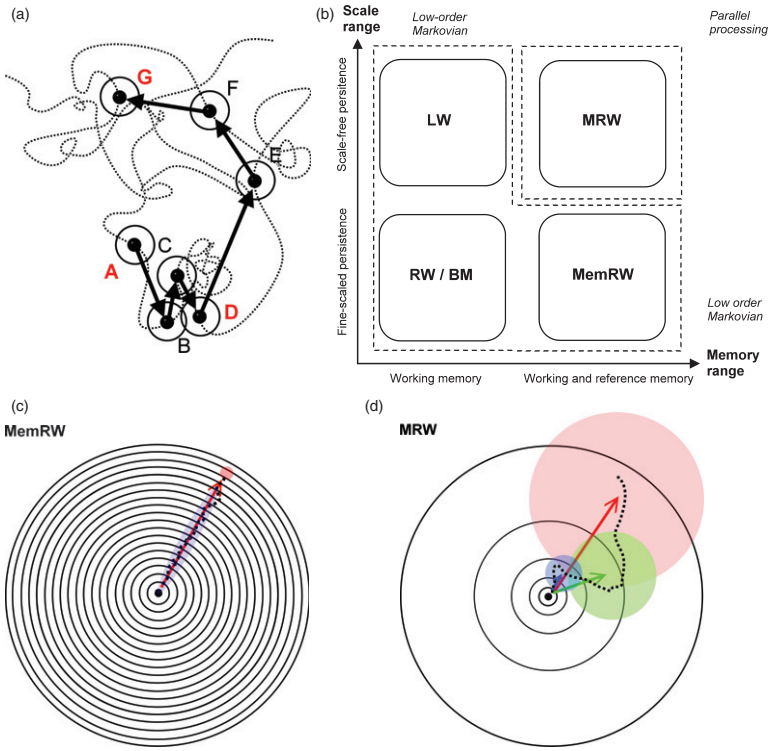

Fig. 1. (a) A hypothetical movement path (dotted line) and a sample of successive relocations of the animal (larger dots) at a fixed time interval Δt illustrates the difference between a mechanistic and a statistical mechanical level of analysis. The circle surrounding each of the relocations represents an animal's perceptual field for current inputs from the environment at a given point in time. First, consider Δt to be sufficiently small to reflect all factors that influence the actual next-step decision, which may also be influenced by previous conditions up to a period of n_w time steps back in time (the animal's memory horizon). If $n_w\Delta t$ is small, the movement may be described in model terms as a low-order Markovian space use process. Next, consider the situation where the relocation interval is increased substantially, to a temporal scale that supersedes the 'Markov limit' $n_w\Delta t$. Each of the successive step vectors at this coarser scale (marked by arrows) will then reflect the summation of many independent substep vectors. Hence, directional persistence is gradually decreased as the relocation interval is increased. Short-term memory becomes embedded in the substeps, and this coarser-scale path may in model terms be described as a Brownian motion (RW). Finally, consider that the observation interval is much larger than $n_w\Delta t$ (or if we use a subsample A, D, G, …). We are then studying the space use at the 'statistical mechanical' level Δt. If n_w for the actual animal is small, the process at this coarsened level is memory-less. On the other hand, if n_w is large, the animal does not satisfy a RW in statistical mechanical terms (since $n_w\Delta t$ – determined by the animal's cognitive capacity – cannot be superseded within the total sampling period). Consequently, an alternative movement class has to be invoked to model space use under a premise of long-term memory. (b) Statistical mechanical variants of space use may be organized along two independent dimensions with respect to their underlying micro-scale mechanistic behaviour, but observed at the coarser temporal lag characterizing statistical mechanics. The four defined classes represent arbitrarily defined discrete intervals over a continuum from approximately scale-specific to (theoretically infinite) scale-free movement, and over a continuum from no memory or short-term memory (working memory-influenced movement; remembering over a short or narrow time horizon) to a mixture of working and reference memory (remembering over a broad, and potentially infinite, time horizon). The combination of scale-free space use and long-term memory (MRW) is postulated to require parallel processing – a spatio-temporal expansion of the low-order Markovian framework (see Supporting Information, Appendix S1 for further details). (c) The Markov compliant processes RW and MemRW are being presented at mechanistic level, that is, assuming time-scale Δt, which defines the average residence time within a spatial grain of magnitude Δr^2 (black centre dot) when the animal is on the move. Let Δr^2 represent the individual's approximate perceptual field. Assume that the average ratio $\Delta r^2/\Delta t$ captures the essence of RW movement and $\Delta r/\Delta t$ captures MemRW as a result of directional bias towards the pink dot. Each surrounding circle from the indicated starting point has an incrementally increasing radius $\approx n\Delta r$, that is, it takes a period of $\Delta t' \approx 18\Delta t$ to reach the pink dot from approximately unidirectional movement (e.g. from MemRW), given no intermediate interrupt of the given bias during this period of time. With no directional bias (RW), the time to reach the circle the pink target resides on is expected to increase to $\Delta r^2/\Delta t = 18^2\Delta t$, from the diffusion law that mean square deviation expands proportionally with time. However, the dot is only one of many potential patches at this distance (circle). Hence, the probability to hit the pink target during $18\Delta t$ is infinitesimal relative to the probability under MemRW. (d) MRW is postulated to simulate a scale-free 'parallel processing' kind of memory-enhanced movement process, where Δr and Δt is expanded by ability to coarse-grain the memory map information in a hierarchical, power law–like manner (in this example, by power of 2: next larger circle is twice the size in linear terms). The respective circles in this cognitive scaling hierarchy are all representing the closest 'neighbourhood-distance' to the individual's current location at different levels of coarse graining. In other words, each circle represents a neighbourhood as cognitively perceived from the perspective of the respective scales. Conceptually, from the perspective of this coarse scale, the centre of the pink area is just a 'neighbourhood-distance' away, but a large distance away from the perspective of lower levels in the cognitive hierarchy of memory-dependent information. Owing to the difference in process rate between the levels (many short-term move decisions and successively fewer larger ones, on average), goals at different levels may be executed relatively independently.

RW, correlated RW and LW are scale specific and with short-term memory only (Markovian). Hence, a LW is also expected to experience direction-influencing events in a manner which will tend to reduce the occurrence of very long steps. Consequently, the chance for long-distance movement with a consistent directional persistence is therefore limited in a heterogeneous habitat. On the other hand, a major difference between RW and LW in addition to the distribution of step lengths is that LW generates a less 'space-filling' path due to the potential for very long displacements. There is a recent controversy surrounding these topics (Edwards *et al*. 2007; Viswanathan *et al*. 2011; Humphries *et al*. 2012; Sims *et al*. 2012), summarized in (Supporting Information, Appendix S1). However, the majority of the recent empirical studies conclude that power law compliant movement is a common phenomenon among a broad range of species and taxa (Viswanathan *et al*. 2011; Sims *et al*. 2012).

Models simulating LW are either based on the short-term working memory (Markovian) kind of process described above (Viswanathan *et al*. 1999; Bartumeus & Levin 2008; Reynolds 2010), or a LW-like pattern is assumed to emerge from a long-term memory-dependent cognitive process involving parallel processing, that is, separate movements decisions running in parallel over a continuum of process rates (Gautestad & Mysterud 2005, 2006, 2010a; Gautestad 2011). In the latter case, called 'multi-scaled Random Walk' (MRW), movement decisions made at various scales are postulated. This implies that animals may take long-distance choices ('strategic decisions') with less interference from the succession of local interrupts ('tactical decisions'). For example, an animal that makes a decision to reach a specific (near or distant) location later in the day may still maintain this goal despite execution of intermediate movement-influencing behaviour (for example, at a minute-to-minute scale). Pre-disturbance (strategic) goal is – under the parallel processing premise – not necessarily erased by the more frequently occurring (tactical) moves at short- and medium scales relative to the large-scale goal. The animal may be 'back on track' after the interruption has faded. This increases the chances of reaching the original target and may thus lead to higher frequency of long-step lengths relative to LW. This resembles hierarchical choice in the empirical literature (Senft *et al*. 1987).

The parallel processing property that is postulated for memory implementation in the MRW model contrasts with the serial (sequential) processing of successive steps (Markovian) exemplified in Fig. 1a. Parallel processing implies a potential for scale-free and continuous distribution of process rates, leading to a power law scaling of observed space use (e.g. measured by the distribution of step lengths or the spatial scatter of GPS locations. Power law distributions are closely linked to fractal geometry (Sugihara & May 1990), which will be a key concept for our data analysis. The concepts of scaling, movement classes and statistical mechanics are described in more detail in Supporting Information, Appendix S1.

In the present study, we approach how the study of animal space use with theoretical movement models can face two separate challenges, related to long-term memory and scaling (Fig. 1b–d; see also a more extensive description of the four space use classes in Appendix S1). Due to the strong empirical evidence of site fidelity in large mammals, as well as seemingly occasional long-distance directed movements, we identify this as key issues when analysing movement patterns based on GPS data. We here present a comparison of statistical patterns in spatial data derived from 4 classes of statistical mechanical movement models with those observed from a data set of GPS fixes from 52 female red deer (*Cervus elaphus*) in Norway. We illustrate statistical patterns of space use that is generated by (1) Random walk (RW, including Brownian motion and correlated RW), (2) LW, (3) MemRW and (4) MRW. These models can be classified along two axes of behaviour: memory and scaling (Fig. 1b). We then compare patterns from these four classes of theoretical movement models (representing the two-dimensional scaling/memory continuum) – by applying three statistical protocols to space use patterns – to those of red deer space use recorded by aid of GPS. Protocols 1–3 are all aimed at estimating the fractal dimension (D), both with the common step length approach (Protocol 1), as well as with a box count approach (Protocol 2) and a hybrid spatio-temporal approach (Protocol 3). The fractal dimension is used to separate the four models along the memory dimension (RW/MemRW) and the scaling dimension (RW/LW). With respect to the RW/LW continuum Protocol 1 is the most frequently used in the literature (Sims *et al*. 2008; Viswanathan *et al*. 2011). We also use other protocols, to achieve more reliable estimates of D from complementary analyses. Protocol 3 provides a test for site fidelity, which is important to separate RW/LW from memRW/MRW (the memory issue). We then see how the real movement data fit into this setting for inferring likely underlying behavioural mechanisms of movements in red deer.

Material and methods

STUDY AREA

The study area is in Sogn og Fjordane county at the western part of southern Norway. The vegetation is mostly in the boreonemoral zone (Abrahamsen *et al*. 1977). Forests are dominated by deciduous (mainly birch *Betula* sp. and alder *Alnus incana*) and pine forest (*Pinus sylvestris*). Norway spruce (*Picea abies*) has been planted in many areas (Mysterud *et al*. 2002). The terrain is characterized by valleys and mountains from coastal to inland areas. Red deer is the most common cervid in the area. In addition livestock, in particular sheep, is common in some

areas. More detail description of the habitat can be found elsewhere (Mysterud *et al.* 2002).

RED DEER DATA

The GPS data come from 52 female red deer caught by darting at winter feeding sites during 2005–2008. The procedure for capture was approved by the Norwegian national ethical board for science ('Forsøksdyrutvalget', http://www.fdu.no). The deer were fitted with Televilt Basic 'store-on-board' GPS (Global Positioning system) collars or Televilt Basic GPS collars with GSM (Global System for Mobile communications) option for transfer of data via cell phone network (Televilt TVP Positioning AB, Lindesberg, Sweden) (Rivrud, Loe & Mysterud 2010). The GPS collars were programmed to record hourly positions, and to release a drop-off mechanism after approximately 10 months (tracking period ranged from 6 to 12 months). The median location error for our GPS collars was 12 m [upper 95% CI = 23 m; (Rivrud, Loe & Mysterud 2010)]. We removed points located further than 10 km from the preceding location ($n = 85$; 0·024% of all points), because they most likely represent large GPS errors and not true deer locations. We here use data from the summer period from 1 June to 16 September. Biologically, this means the period when individuals are in their summer range and when most adult females give birth to a calf. During this period, red deer in similar landscapes in the Alps spent > 50% of the time foraging (Georgii 1981), while a major part of the inactive time is spent ruminating and resting. Calving status of the marked female red deer was unknown, but most adult females ovulate and are likely accompanied by a calf (Langvatn *et al.* 2004). The end of the period coincides with the onset of hunting season (from 10th September), fall migration (Mysterud *et al.* 2011) and rutting activities (Loe *et al.* 2005). Seven animals were still in migration phase and fixes from this period were discarded from the analysis [as in Rivrud, Loe & Mysterud (2010)].

FRAMEWORK TO COMPARE FIXES FROM SIMULATION MODELS AND REAL DATA

Due to the coarser-scale $\Delta t'$ that is invoked in a statistical-mechanical approach to model animal space use (see *Introduction*), a given GPS pattern's fractal properties may distinguish between the four movement classes in Fig. 1b. While classical Euclidian geometry describes natural objects in 0-, 1-, 2- or 3-dimensional space (i.e. integer-dimensional), fractal geometry describes objects that are not 'scale-specific' but require a fractional dimension to be quantified and analysed more precisely. For example, a coastline that is rugged over a range of scales has a resolution-dependent length, like $100\ km^{1.2}$ instead of $100\ km^{1}$, where $D = 1{\cdot}2$ and 100 km is the length when measured from a specific resolution (the divider's width or pixel size of the map from which 100 km was calculated). From the magnitude of D, it is easy to estimate the expected change of length at an alternative resolution, while a nonfractal object (like a highway) would not change its lengths at different scale. The highway's length is clearly not expected to change whether it is measured in metres or kilometres. On the other hand, an animal's rugged path is – if it has fractal properties – more precisely described by D than by a Euclidian length, and for example, the number of virtual grid cells (representing the observer's choice of 'pixel resolution') that is found to be visited after collecting N spatial relocations may be better described by D than an Euclidian area (sum of visited grid cells). If $D < 2$, the area will depend on both the grid resolution and N. We refer to Sugihara & May (1990) for a general introduction to fractals in a biological context.

All four movement classes in Fig. 1b are in their respective generic forms characterized by a scale-free (self-similar and statistically fractal) kind of space use over a broad range of boundary conditions, but RW and MemRW generally lead to a larger fractal dimension, D, than LW and MRW (Gautestad & Mysterud 2010a). For example, while a Brownian motion-like RW path will appear relatively convoluted with relatively small variance of lengths between successive step lengths, a LW path will show a much broader range of step lengths and – consequently – show a less space-filling path (smaller D) due to the occasional large steps that bring the animal to relatively distant locations.

Statistical protocols to estimate D within the framework of Fig. 1 have already been described and tested in simulations (Gautestad & Mysterud 2005, 2006, 2010a,b; Gautestad 2011). Three of these protocols are applied below to determine which of the four classes that provides the best compliance with the actual red deer space use. D is estimated either from a multi-scale analysis of an individual's movement path (a 'Lagrangian' approach; from studying the path properties) or a multi-scale analysis of the spatial scatter of fixes (an 'Eulerian' approach; a spatially explicit analysis).

Simulation results with respect to the respective movement classes' expected range of D are summarized in Table 1. A conceptual summary of the expected statistical patterns from all four classes, based on the three present protocols to estimate D, are shown in Fig. 2.

PROTOCOLS FOR COMPARING SPACE USE DATA

As a fractal dimension varies over a continuum, estimates of D provide a first approach to test for compliance with the respective movement classes at a statistical mechanical level of observation. Between three of the four defined movement classes in Fig. 1b, there is no or little inter-class overlap of respective ranges of D according to simulations. All four classes can be distinguished by supplementing estimates of D with a test for area containment of space use due to memory influence, that is, a

Table 1. Expected ranges of the fractal dimension D for four main classes and five subclasses (variants) of simulation models: classic random walk, Brownian motion and correlated random walk (RW), Lévy walk with $\beta = 2$ (LW), RW with fixed memory horizon ($MemRW_{memfix}$), Multi-scaled random walk with $\beta = 3$ ($D_{STEP} = 2$) and fixed memory horizon ($MRW_{memfix3}$), MRW with $\beta = 2$ and fixed memory horizon ($MRW_{memfix2}$), RW with infinite memory ($MemRW_{inf}$), MRW with $\beta = 3$ and infinite memory (MRW_{inf3}) and MRW with $\beta = 2$ and infinite memory (MRW_{inf2})

Movement class	Conceptual (M = memory, SS = spatial scaling)	Range of D (from simulations)	Site fidelity	References to theory and simulation results
RW	M: no SS: no	$1{\cdot}5 < D < 1{\cdot}7$	No	Mandelbrot (1983), Sugihara & May (1990)
LW	M: no SS: yes	$0{\cdot}9 < D < 1{\cdot}3$	No	Mandelbrot (1983), Hagen *et al.* (2001)
$MemRW_{memfix}$	M: limited SS: no	$1{\cdot}5 < D < 1{\cdot}7$	No	Appendix C
$MRW_{memfix3}$	M: limited SS: yes	$1{\cdot}4 < D < 1{\cdot}5$	No	Appendix C, Gautestad & Mysterud (2010a)
$MRW_{memfix2}$	M: limited SS:yes	$0{\cdot}9 < D < 1{\cdot}3$	No	Gautestad (2011), A. O. Gautestad (unpublished results)
$MemRW_{inf}$	M: yes SS: no	$1{\cdot}5 < D < 1{\cdot}6$	Yes	Appendix C
MRW_{inf3}	M: yes SS: yes	$1{\cdot}3 < D < 1{\cdot}4$	Yes	Gautestad & Mysterud (2010a)
MRW_{inf2}	M: yes SS: yes	$0{\cdot}9 < D < 1{\cdot}3$	Yes	Appendix B; Gautestad & Mysterud (2005, 2006, 2010a)

home range emerging from site fidelity. With reference to Fig. 1b, both the scaling dimension and the memory dimension are needed to separate the two classes LW and MRW.

Protocol 1

Protocol 1 regards the Lagrangian approach to the data, by studying the scaling properties of the long-tail part of a binned step length distribution, $F(L)$, of successively observed displacements of an individual at observation intervals (lags) in the domain of spatial autocorrelation [see Swihart & Slade (1985) for a description of the autocorrelation property in a home range context]:

$$F(L) = \alpha L^{-\beta} \Big| L < \lambda \qquad \text{eqn 1}$$

Equation 1 implies a scale-free, that is a power law, relationship between one step length bin (length interval) and the next (Viswanathan *et al.* 2000), as measured over the tail part (L is larger than the median step length, implying that smaller steps fall in the first bin). The truncation scale λ represents the approximate maximum displacement during an interval Δt, and typically reflects a maximum movement speed. Direct environmental constraint on step length (e.g. a 'valley effect' or territorial borders) can also lead to truncation. If β is stable over a large range of L (for example, 10–100 times larger than the smallest class), the distribution satisfies a power law with fractal properties over the given scale range. The fractal dimension of the path, D_{step}, can then be approximated by $D_{step} = \beta - 1$ for $1 \leq \beta \leq 3$ (Viswanathan *et al.* 2000). LW and MRW are typically characterized by $\beta \approx 2$ ($D_{step} \approx 1$), that is, a distribution showing high frequency of short steps and also a presence of very long steps. RW and MemRW (Brownian motion, RW and correlated RW observed at level $\Delta t'$) are characterized by β closer to 3 (D_{step} closer to 2) or typically much larger. In this case, extremely long steps are practically absent. MRW is similar to LW with respect to β and D_{step}, except for a tendency for 'hockey stick' pattern: at very large L, the influence from return steps tend to inflate $F(L)$ relative to expectation from a generic LW distribution. This effect may under some boundary conditions create an extra 'hump' at the fitted slope of the log-log transformed distribution of step lengths over the largest bins of step lengths (Gautestad & Mysterud 2006; Gautestad 2012) (see Appendix S1 for details on how the hockey stick pattern will depend on the ratio between return step frequency and observational lag between successive fixes). There is a close relationship between the Lagrangian parameter D_{step} and the complementary Eulerian parameter D, which describes the scaling properties of the spatial scatter of fixes over the landscape [Hagen *et al.* (2001); see also Protocol 2 and 3 below].

LW is a movement process without long-term memory. Hence, space use constraint is not expected in an open environment owing to lack of directed return steps. Further, step truncation at length scale can in the present context of ungulate space use be expected to take place at fine scales – with a disrupted power law as a result. Hence, in this case, the truncation level typically reflects the average distance to a resource patch. Under strong step length truncation (relatively small λ), Eqn 1 will show a log-log linear relationship only over a narrow range of L, with steeper slope beyond this range. Further, LW does not show homing towards previous locations, and this property can be applied to distinguish LW from

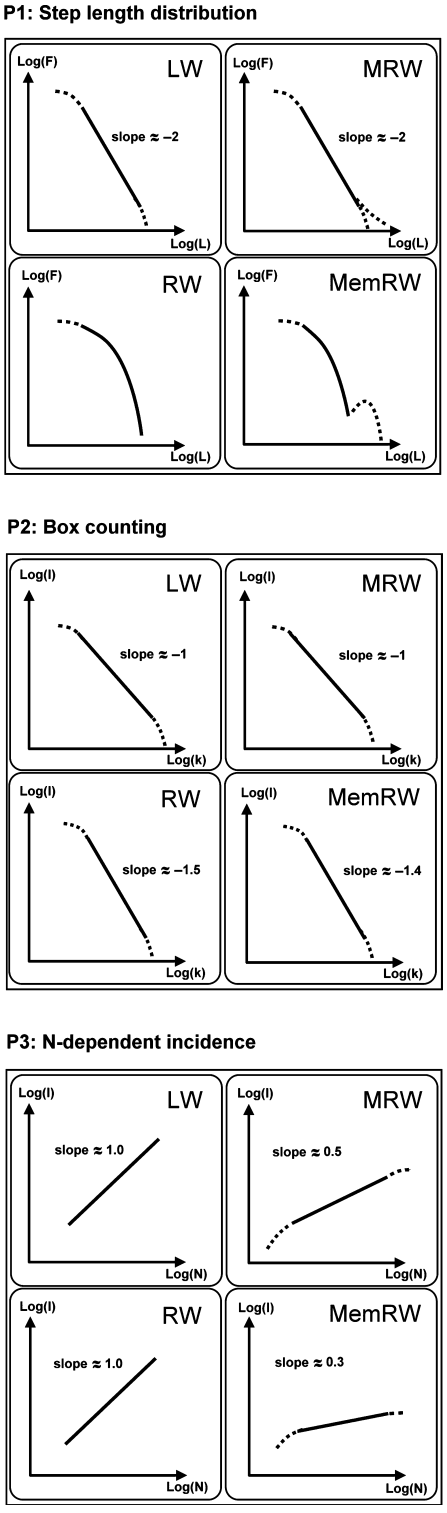

Fig. 2. The three protocols P1–P3 for estimating fractal dimension D are illustrated conceptually, from the respective expected relationship between dependent $\mathbf{Y} = \log(y)$ and independent $\mathbf{X} = \log(x)$ variables, based on previous and present simulation results (see references in Table 1). X represents binned step length L (Protocol 1), spatial resolution k (Protocol 2) and sample size of number of fixes N (Protocol 3). Y represents frequency F (P1) and incidence I (number of nonempty grid cell boxes at resolution k) (P2 and P3). Double-log linearity implies power law compliance, from $\log(y) = \log(a) + b\log(x)$ where a and b are parameters. RW and MemRW are not power law compliant under P1, which means that an estimate of D in these instances is limited to P2 (RW and MemRW) and P3 (MemRW). Continuous lines show the actual model (with typical slope examples indicated), while dotted lines indicate expected nonlinearity either from limits of range of scaling or from statistical artefacts. For example, in absence of step length truncation MemRW and MRW under Protocol 1 may show a tendency to an inflation of steps (a 'hump') in the largest bins due to a mixture of two distributions – exploratory steps and return-biased steps. As Protocol 1 requires autocorrelated series, analyses on MRW and MemRW are requiring observation frequency substantially larger than average return step frequency. The magnitude of the hump (which looks more like a 'hockey stick' for MRW with $D_{\text{step}} = 1$) will increase if observation frequency is set closer to return frequency.

MRW in real data when estimates of D_{step} from Protocol 1 is found to be nonconclusive.

However, truncation effects, which are scale-specific by nature, may interfere with the ideal power law property of a scale-free process also in more subtle ways, as for LW and MRW. For example, both movement speed (displacement pr. GPS fix interval) and the environment (e.g. a valley with steep slopes hindering free movement) may constrain the frequency of extreme step lengths, leading to cut-offs, and thus a steeper slope (larger β) towards the larger classes of step lengths. The larger β may then lead to the impression of a larger D (larger β) than the underlying intrinsic process relative to how it would be expressed in the absence of physically or environmentally imposed truncation. We propose the following supplementary and novel test to cast light on this issue: as power law distributions of step lengths are characterized by a sample-size (N) dependent second moment (nonstationary distribution) (Bouchaud & Georges 1990), increasing N may from this property be expected to show an increased influence from truncation with increasing N. In other words, an intrinsically *scale-free* pattern becomes subject to an increasing influence from *scale-specific* physical or environmental factors when the tail part of the distribution increases as a function of N. Conversely, a truncation effect on β should be expected to diminish when reducing N. Thus, by splitting a large N series into sections containing smaller N and averaging over the subsamples, a better interpretation of nonlinearity in double-log plots of step lengths may be achieved if inflation of the exponent β *with increasing* L in Eqn 1 is linked to environmental constraint. This supplementary analysis will thus be performed on the red deer data.

The fix collection period of one summer season covers both phenological dynamics and habitat heterogeneity. However, similarly to a physical Brownian motion particle traversing spatial subsections with locality-specific movement speed and turning frequency (due to, for example, differences in viscosity and frequency of interparticle collisions), the particle's overall path during a period T will still describe a Brownian motion. For

example, in Fig. 1a, the hypothetical path of an individual describes locally varying movement speed and directional persistence, for example as a result of local habitat heterogeneity. However, because the step lengths under study have been sampled over a large period T (and assuming that the relocation interval for fix sampling is sufficiently large to ensure a statistical mechanical level of analysis), the overall properties of the step length distribution are reflected in the average values like median step length, median level of directional persistence (path auto-correlation) and other statistics. Hence, from a hypothetical collection of a set of N observed relocations of the animal, collected at fixed intervals during T, one finds the average movement constants and parameters for hypothetical subsets of fixes that could alternatively be collected over subsections of T or specific subranges of the total range. The latter approach would then express the intra-T and intrarange heterogeneity of the individual's space use conditions. This principle is recently adjusted and applied to study intra-home range habitat heterogeneity (Gautestad & Mysterud 2010b; Gautestad 2011) and phenological effects on space use (Gautestad & Mysterud 2006), both in the context of statistical mechanics and the fractal dimension D. In the present analysis, the respective individual red deer's space use is analysed in overall terms only; that is, we are studying the average scaling properties (as expressed by β and D) over the extent of one season and the observed area traversed during this season.

Protocol 2

Protocol 2 is based on a fractal analysis of the spatial distribution of fixes. Thus, the focus is shifted from a Lagrangian (Eqn 1) to a spatially explicit Eulerian analysis of space use. An analysis of D from a simple 'box counting method' (Feder 1988), as outlined below, may reveal to what degree an individual has performed space use in compliance with one of the four movement classes in Fig. 1b. Consider a set of imaginary grids of different linear grid cell size k that are superimposed upon an area of size δ^2 containing all observed fixes (δ^2 is set to be equal to or larger than this home range), where – starting for the finest resolution – the next and coarser-grained grid has k^2 larger grain (grid cell area) and k^{-2} as many grid cells and thus k^{-2} as many degrees of freedom for inter-cell movement. The number of grid cells containing at least one fix within the extent δ^2, defined as incidence, I, can then be expressed as a function of k (Gautestad & Mysterud 2005, 2006, 2010a):

$$I(K) = \delta k^{-D} | k \leq \delta; \delta \equiv 1 \qquad \text{eqn 2}$$

D represents the spatial fix pattern's fractal dimension, which is statistical of nature in this context. In broad terms, $D \approx D_{\text{step}}$ (Hagen *et al.* 2001; Gautestad & Mysterud 2010a). Eqs. 1 and 2 can consequently be considered alternative methods to estimate D. A site fidelity pattern that is generated by memory-less RW (thus, space use is assumed to be constrained by environmental factors) is expected to show $1{\cdot}5 <\approx D <\approx 2$ at scales $\Delta t'$, while MRW shows $D \approx 1$ (i.e. of similar magnitude as D_{step}), except for an influence of statistical artefacts that become prominent at very small and very large k relative to δ (Gautestad & Mysterud 2012). These artefacts are due to the constraints that for very large grid cells all fixes will be in one square (the entire home range), while for very small grid cells one will end up with either one fix or no fix. Clearly, intermediate grid cell sizes between these extremes are most suited for inference.

Memory enhanced random walk in the form of biased and correlated RW with memory-influenced return steps at mechanistic scale Δt (*sensu* Börger, Dalziel & Fryxell 2008 and Van Moorter *et al.* 2009; but in the present statistical mechanical context coarse-grained to a sampling interval larger than Δt) has been hypothesized to show $D >\approx 1{\cdot}5$ (Gautestad & Mysterud 2010a). This is a similar magnitude of D as expected from area-constrained Brownian motion and classical RW.

In summary, an individual that is found to express site fidelity (and thus excluding LW) and where analysis show $1 <\approx D \ll 1{\cdot}5$ (and stable over a range of spatial scales) supports a MRW kind of space use. Home range behaviour with scaling pattern in the transition range $1{\cdot}4 < D < 1{\cdot}5$ may be compliant both with MemRW (Markov compliant) and MRW (non-Markovian) where D_{step} is tuned towards 2 rather than the default $D_{\text{step}} = 1$.

Protocol 3

Protocol 3 investigates how the scatter of fixes expands over space as a function of number of fixes, N, when observed at a given spatial resolution k. For a memory-influenced process observed (at scale t_{obs}) the domain of spatially nonautocorrelated fixes, the N-dependence is again formulated as a power law (Gautestad & Mysterud 2010a):

$$I(N) = cN^{1-D/2} | N_{\min} < N < N\max; k \ll \delta \qquad \text{eqn 3}$$

$N_{\min}$ and $N_{\max}$ represent the transition zones towards specific statistical artefacts' influence on the exponent $z = 1-D/2$ for small and large N, respectively (Gautestad & Mysterud 2010a, 2012). The fractal dimension D can be estimated as

$$D = 2(1 - z) | N_{\min} < N < N\max; k \ll \delta \qquad \text{eqn 4}$$

As the set N is assumed to be collected from the domain of spatially non-autocorrelated fixes [see Swihart & Slade (1985) for a definition], N may be proportional with the successively expanding sampling period T or proportional with an increased sampling frequency during a fixed T.

Under this condition, the observed I for a given N is expected to be of the same magnitude regardless of method to vary N, given that the space use is memory-driven.

Eqn 3–4 also applies for spatially autocorrelated fixes, but only if the N fixes are sampled in a manner, which make N increasing proportionally with T (A. O. Gautestad, unpublished data). This sampling method will be applied for the red deer data, which may be autocorrelated owing to small fix intervals of magnitude one or a few hours.

For a MRW with $D_{\text{step}} = 1$, the exponent z is expected close to 0·5 (Gautestad & Mysterud 2005, 2010a). Hence, $D \approx 1$ is expected (range of D is given in Table 1).

For the sake of completeness with reference to simulation results under the four movement classes summarized in Fig. 1 and Table 1, we have performed novel statistical mechanical simulations both of MRW where the observation frequency of fixes is in the transition zone between autocorrelated and nonautocorrelated fixes (Appendix S2) and of MemRW based on correlated RW (Appendix S3, Supporting Information).

STATISTICAL ANALYSIS OF RED DEER DATA

Each series under analysis consists of one individual red deer's set of fixes from one summer season. Protocols 1–3 were applied to estimate the individual fix series' fractal dimension, D, from the Lagrangian perspective (Protocol 1: step length distribution) and the Eulerian perspective (spatial scatter of fixes, Protocols 2–3). All series consist of at least 1000 fixes each, collected with time lag 1 h, that is, from the domain of potential spatial autocorrelation occurring up to 4-h intervals. The fix interval was larger due to missing positions exceeded 4 h in only 0·6% of the observations.

For the Protocol 1 analysis, only the red deer with the 18 longest time series were selected, to ensure large subseries for analysis both of step lengths from (a) the total series length for each individual, and (b) from eight subseries consisting of steps 1–300, 301–600, … 2100–2400 in each series. The step length histogram for the subseries, representing the average bin scores over the eight series, was then compared with the histogram for the series as a whole for the purpose to study environmentally imposed truncation effect on β (see description of method under Protocol 1 description above).

For the Protocol 2–3 analyses, D was estimated for all 52 red deer. Estimates are with 95% confidence intervals. We analysed the data both as average result from linear regression over all individuals and for each individual separately (Appendix S4, Supporting Information). Piecewise regression was applied to study individual break points, that is, deviations from double-log linearity in the extreme part of the long tail; either in the form of truncation (subabundance of extreme steps) or hockey stick (superabundance of extreme steps). Piecewise regression was conducted with the function 'segmented' in the R package with the same name (Muggeo 2008). Standard least squares linear regression was also performed for comparison. The Akaike information criterion was used to select the best-fitting model (Burnham & Anderson 2002).

To explore potential nonlinear relationships, we used generalized additive models (GAM), modelled with the functions 'gam' and 'gamm' (mixed model extension) in the R package 'mgcv' (Wood 2006). GAM in mgcv solves the smoothing parameter estimation problem using the generalized cross-validation (GCV) criterion, which in effect is a built-in test for linearity (i.e. the presented nonlinear plots fits the data statistically better than competing linear fits and vice versa). GAM was used to explore nonlinearity for Multi-scaled RW and Memory-based RW (with $D_{\text{step}} = 2$) in Protocol 1–3 (Appendix S3 Fig. C1e–g) and to explore the effect of lag (in hours) on distance moved in red deer (Appendix S5 Fig. E1, Supporting Information). Inclusion of random effects and modelling of heteroscedasticity follows (Zuur *et al.* 2009) and is presented specifically in each case.

Direct linear regression and piecewise regression of log transformed step length distributions are supplemented by maximum-likelihood estimates (MLE), which is recommended for analyses in the context of Protocol 1 (Edwards *et al.* 2007; Edwards 2008). Three choice models were fitted to the 18 largest series; power law, truncated power law and exponential. Method details are given in Appendix S5.

Results

The fractal dimension (D) estimated from the simulations based on RW, MemRW, LW, and MRW models were similar in all 3 protocols and were close to the theoretical expectations (Table 1). Figure 4 summarizes the results from the red deer GPS data compared with ranges from simulations with the four classes of theoretical models using all three protocols to estimate fractal properties of space use. In the following, we detail how the overall red deer space use fit with the various theoretical models using each of the three statistical protocols, while we in Appendix S5 present detailed analyses of each individual red deer time series.

PROTOCOL 1 – ESTIMATING D FROM STEP LENGTHS

The step length histogram for the 18 female red deer during the summer season showed tendency for a nonlinear slope in a log-log transformation of axes (Fig. 3a). Over the smaller bins 80–880 m ($\log_2$ values from 6·32 to 9·78), the regression line indicates a power law with slope $\beta = -2{\cdot}14$, which estimates the fractal dimension over this scale range to $D = 1{\cdot}14$. However, the slope steepens towards larger step lengths. Hence, the series were split into subsamples of 300 fixes each to test the hypothesis

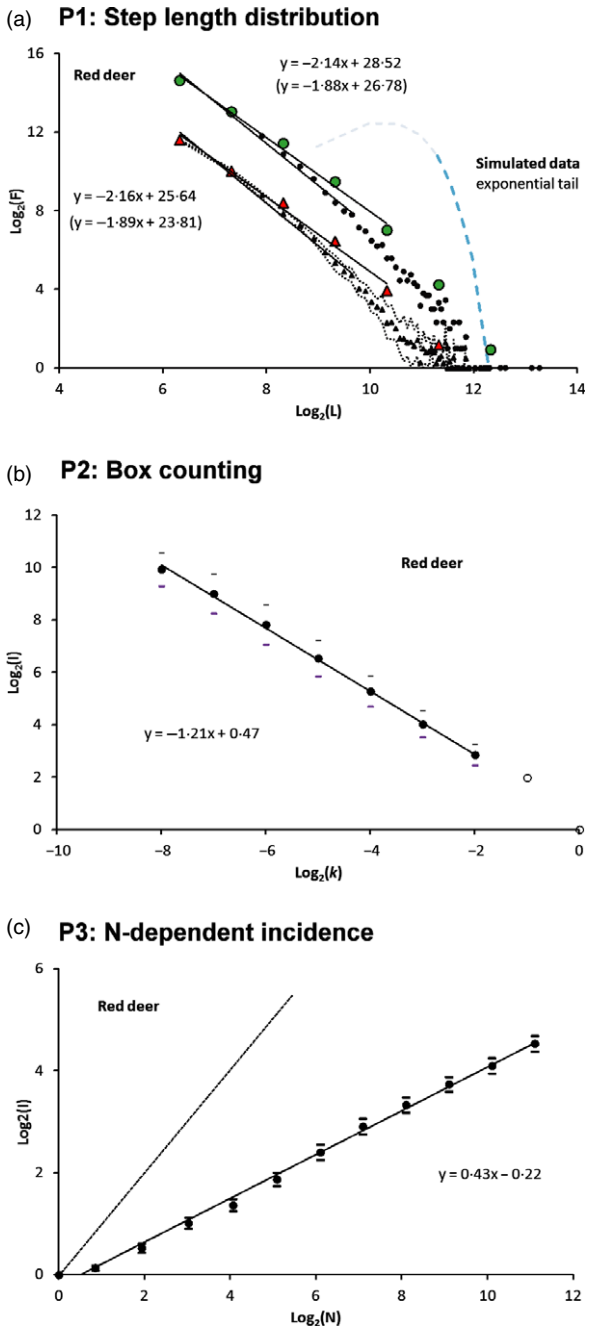

Fig. 3. (a) Protocol 1 applied on the red deer data: Log-log transformed scatter plot of bin-classed distribution of step lengths, from individual sets of GPS summer fixes from the 18 largest series (circles). Each bin class represent increments of 80 metres, and bin scores for the respective individuals are averaged. A power law-like compliance is seen over some range of the plots (filled circles), with slope −2·14. This translates to $D = 1{\cdot}14$ (see main text). When the respective series are split into eight subseries of 300 steps and then averaged over 18*300 subseries (triangles; ± one standard deviation shown as dashes), the compliance with a power law improves over the largest bin classes. For comparison, a step length distribution from a simulated Brownian motion series (characterized by a negative exponential rather than a power law tail; black dotted line; ref. Fig. 2) shows a much steeper slope for the largest bin classes. The tail part fits the function $\ln(y) = -0{\cdot}0047x + 23{\cdot}85$. (b) Protocol 2 (box counting) applied on respective GPS fix series from 52 female red deer and then averaged per bin shows log(k,I) scores in compliance with a scale-free kind of movement like Lévy walk and MRW, with negative slope −1·21 of the distribution. This implies $D \approx 1{\cdot}21$. The smallest log(k,I) values were excluded from analyses (open symbols), due to influence from statistical artefacts. (c) Protocol 3 applied on the 52 GPS series, with spatial resolution $k = 1 : 10$ relative to respective series' arena sizes, gives a consistent log-linear slope $z = 0{\cdot}43$ over a broad range of fix sample size, N. This translates to $D = 1{\cdot}14$. Least square linear regression was used for the slope, and ±1 standard error for 51 degrees of freedom is shown as dashes above and below each (N,I) plot (independently calculated pr plot).

that this is a truncation effect of physical or environmental origin on an otherwise scale-free process. When each of the 18 series was split into eight subseries of 300 step lengths, the slope was still approximately linear on average over the same bin range ($\beta = -2{\cdot}15$; $D = 1{\cdot}15$), but the nonlinearity in the tail part was reduced – an indication of a truncation effect (ref: description in relation to Eqn 1 above).

Consequently, even if the result in Fig. 3a was not fully compliant with a power law in its ideal statistical form (log linearity over a broader range of bins), the distribution was very distant from the expectancy of strong nonlinearity in double-log plots (absence of a power law pattern) from MemRW based on correlated RW (ref. concept in Fig. 2, simulated exponential tail in Fig. 3a and simulation results in Appendix S3). Further, the MLE log-likelihood ratio parameters for power law (generic LW) vs. truncated power law gave strong support for power law vs. truncated power law and exponential function for 15 of the 18 individuals (Appendix S5, Table E2a and E2b). The 'straightening-out' of the double-log regression line after splitting the series into subsamples of smaller N also supports a scale-free space use process by the red deer.

When analysing the full series based on piecewise regression (Appendix S5), a truncated model fitted the data better than the generic linear form for nine of the 18 individuals' full series. The average break point for truncation was 28·89 = 474 m. On average, $\beta = 2{\cdot}17$ (SE = 0·0676) for the best-fitting model versions (using the first-range slope for individuals were the piecewise regression gave the best goodness of fit). This translates to a spatial fractal dimension estimate $D \approx D_{\text{step}} = 2{\cdot}17 - 1 = 1.17$. However, none of the individuals showed a strong deviation from general linearity. The average β from standard linear regression was 2·41 (SE = 0·0537) and $D = 1{\cdot}41$. This could be due to the truncation effect, which makes the overall slope steeper (see Appendix S5 Fig. E1a for graphical presentations of the individual plots). The MLE did generally not confirm the truncation effect as clearly as the visual inspection indicated and the piecewise linear regression analyses supported. The average full series estimate of β from MLE was 2·31 for truncated LW, which is somewhat larger than the average result $\beta = 2{\cdot}17$ from piecewise regression but smaller that the result from stan-

dard linear regression. MLE also supported LW with a strong log-likelihood parameter −83·47 on average. However, the MLE approach has not been developed and theoretically adjusted for the MRW kind of model, which may lead to a truncation-absorbing 'hockey stick' pattern in the step length distribution (Appendix S2: Discussion of the hockey stick).

Thus, the results under from Protocol 1 are within the range of both MRW and LW and outside the range of RW and MemRW (Table 1; Fig. 2), providing support to the hypothesis that red deer space use involves parallel processing of multiple scales (Fig. 1d).

PROTOCOL 2 – ESTIMATING *d* FROM BOX COUNTS

The fix series from the total set of 52 individuals revealed a fractal pattern over a scale range of 1 : 4 1 : 128 or 1 : 256 relative to respective arena size categories (Fig. 3b), with $D = 1{\cdot}21$ when the two coarsest resolution plots were excluded (95% CI, $-1{\cdot}15 < D < 1{\cdot}26$), $D = 1{\cdot}22$ otherwise (95% CI, $-1{\cdot}15 < D < 1{\cdot}29$). When analysing each individual separately piecewise regression gave best fit for 32 of the 52 series, with slope -1·02 (SE = 0·0309) on average for the respective best-fit models (Appendix S5). For the standard regression model, slope was =−1·21 (SE = 0·0134). The respective estimates of fractal dimension was thus $D = 1{\cdot}02$ and 1·21, respectively. Thus, the results of Protocol 2 are, as for Protocol 1, within the range both of MRW and LW, and outside the range of RW and MemRW (Table 1; Fig. 2a–b).

PROTOCOL 3 – ESTIMATING *d* FROM SAMPLE SIZE-DEPENDENT INCIDENCE

Incidence as function of number of fixes N, calculated at grid resolution $k = 1 : 10$ relative to respectively defined arena sizes and averaged over all 52 series, revealed a close compliance with a power law (Fig. 3c). The average exponent $z = 0.43$ (95% CI, $0{\cdot}41 < z < 0.45$) translates to $D = 1{\cdot}14$ (95% CI, $1{\cdot}10 < D < 1{\cdot}18$) according to Eqn 4. The regression slopes for other grid resolutions were of similar magnitude, but over a smaller range of N due to statistical artefacts when calculating z at large resolutions (small k) in combination with small N (see Appendix S4 for details). The range of observed slopes z is closely compliant with MRW and clearly noncompatible with LW and RW (for which z closer to 1 is expected; Fig. 2c). It is also substantially different from MemRW (expectancy of z in range, 0·2–0·3 and thus $1{\cdot}4 < D < 1{\cdot}6$). For example, 20 simulated series or MemRW under condition of correlated RW with return steps gave average $z = 0{\cdot}27$ (95% CI, 0·24–0·30) (Appendix S3).

When analysing each individual separately, Protocol 3 revealed a relatively strong interindividual variation in (non)linearity of $\log(I)$ as a function of $\log(N)$. However, on average the slope was $z = 0{\cdot}40$ (95% CI, 0·34–0·46) for the best-fit models and $z = 0.41$ (95% CI 0·36–0·46) for the standard regression alone. These results translate to $D = 2(1-z) = 1{\cdot}20$ and 1·18, respectively.

Figure 4 summarizes the results from the red deer data, and compares the parameter estimates under the three protocols with the theoretical ranges in Table 1. More detailed results for the analysis of individual series are described in Appendix S5.

Thus, the estimates of the fractal dimension in red deer space use from Protocol 3 are within the range of only MRW (Fig. 4) and outside the range of the MemRW. For the memory-less LW/RW a slope z close to 1 in a log (I,N) plot is expected (area in the form of incidence expanding approximately proportionally with N, i.e. time). Thus, even if Eqns. 3–4 under Protocol 3 cannot be applied to estimate D for memory-less space use like RW

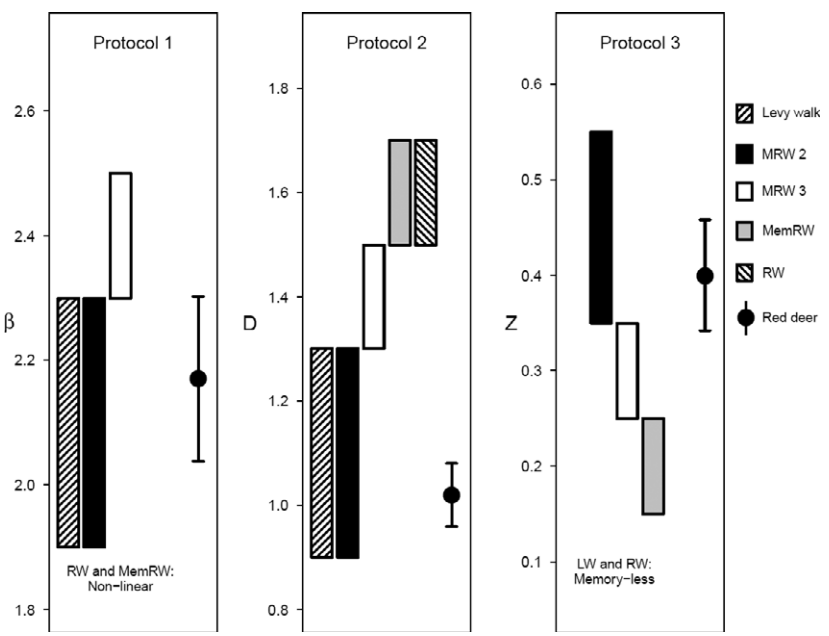

Fig. 4. Comparison of parameter estimates (with 95% confidence intervals) from red deer GPS data under Protocol 1 (β), Protocol 2 (D) and Protocol 3 (z) relative to theoretical ranges of D from Table 1. Transformation of the exponents β and z to D are explained in relation to Eqns 1 and 4 in the text: $D_{step} = \beta - 1$ implies that $\beta = D_{step} + 1$, and $D = 2(1-z)$ implies $z = 1 - D/2$. Autocorrelated series are required for analysis under Protocol 1. MemRW and RW do not produce power law distribution of steps, and β under Protocol 1 can consequently not be estimated. Under Protocol 3, LW and RW do not produce $z \ll 1$ due to lack of memory and site fidelity, and Eqn 4 can consequently not be applied.

and LW, a large z close to one will reveal an absence of memory-dependent site fidelity.

Discussion

Linking individual movement to animal space use patterns has been highlighted as a key research theme (Börger, Dalziel & Fryxell 2008). We here provide one such link by comparing the statistical patterns of set of fixes from simulation models of animal space use with GPS data from 52 female red deer (Table 1). The basis of the different simulations models, RW, LW, MemRW and MRW are assumptions used to mimic different animal behaviours (Bartumeus & Levin 2008; Gautestad & Mysterud 2010a). When analysed at a statistical mechanical level, which is most relevant when comparing to GPS location data (see *Introduction*);that is, we have categorized all models at this level under four main movement classes depending on presence of memory (return steps) and degree of scale-free movement (Fig. 1b). We found that the statistical pattern of red deer space use was closer to the LW/MRW models than RW/MemRW based on the fractal dimension D from all three protocols (Fig. 4). Further, the appearance of area-constrained space use (home range) supports MRW over LW-like space use and MemRW over RW. We thus infer that both the underlying behavioural processes – long-term memory and scale-free movement (Fig. 1), that is, the presence of both strategic and tactical movements, are consistent with the observed red deer space use as recorded with GPS.

CONSTRAINED SPACE USE – EVIDENCE FOR MEMORY?

Most behavioural ecologists would agree that mammals use some kind of spatial memory (Piper 2011). Indeed, the presence of such structures has been shown experimentally in brain research (Hafting *et al.* 2005). How to empirically infer memory-based space use from GPS or other movement data is less obvious. A higher use of previously visited habitats than expected from random encounter has been one approach (Wolf *et al.* 2009), but simulations suggest problems with this approach if habitat models were incomplete (e.g. hidden resources or inaccurate habitat maps) as would be the case for most field studies (Van Moorter *et al.* 2012). Here, we have applied an alternative approach, derived from an expansion of classical statistical mechanics to account for scaling and memory effects, and compared properties of simulated space use data to those of red deer.

Lack of long-term memory influence, that is, a Markovian kind of movement, will in this scheme lead to nonconstrained movement. However, constrained space use *per se* is not necessarily indicative of spatial memory. For example, conspecific aggression may in theory chase any red deer back to the home range of the individual or the matrilinies. If so, a home range may be maintained as a mixture of the effect from territorial aggression and memory. Landscape constraint on space use (fiords or mountains in our case) may also affect the results, as may be indicated by the full series results in Fig. 3a, in addition to direct visual inspection of the respective spatial scatter of fixes. With respect to Protocol 3, an asymptotic approach towards a stable area as sample size of fixes increases should become apparent if the home range was due to a memory-less movement process (RW and LW) and environmentally constrained. However, we found no empirical evidence for such an asymptote (Fig. 3c).

Further, simulations have shown that D is found to increase significantly when any of the four movement classes in Fig. 1b is subject to environmental area constraint (in all cases, resulting in $D > 1{\cdot}5$; that is, a more space-filling scatter of fixes, even for MRW with $D \approx 1$ under unconstrained space use) (A. O. Gautestad, unpublished data). These considerations, together with the consistent power law compliance ($D \ll 1{\cdot}5$) for the red deer data under all three protocols (Fig. 4) imply that range constraint due to territorial behaviour or other environmental factors is unlikely to be the mechanism underlying the observed space use. On the contrary, the results support home ranges as an emergent property from an intrinsically driven memory process. This is what is expected also based on knowledge of the social organization for this particular species. There is clear evidence that related female red deer share ranges to a larger extent (Clutton-Brock, Albon & Guinness 1982; Coulson *et al.* 1997), which has also been found in many other mammals (Comer *et al.* 2005). This implies that no clear repellence effect relative to individuals in the neighbourhood is expected, apart from individuals at the periphery towards other matrilineal groups. It would clearly be interesting to pursue this issue for species and under conditions in which territorial behaviour is a likely driver of home range extent, like in many large carnivores (Jędrzejewski *et al.* 2007), birds (Rhim & Lee 2004) and also for male red deer under some environmental conditions (Carranza, Alvarez & Redondo 1990; Carranza, Garcia-Munoz & de Dios Vargas 1995).

CONTEXT-SPECIFIC SITE FIDELITY

The recent verifications of LW-compliant behaviour have been particularly based on studies of marine animals, where pelagic search conditions may facilitate this kind of opportunistic foraging where resources are relatively scarce (Sims *et al.* 2008; Humphries *et al.* 2010; Hays *et al.* 2012; Humphries *et al.* 2012; Sims *et al.* 2006, 2012). Homing and site fidelity may not provide fitness gain where resources are sparsely and unpredictably distributed, because the old information in the memory base becomes swiftly outdated. On the other hand, use of memory strategically (as modelled in MRW) may be expected only under ecological conditions that support site fidelity: high-resource abundance with a relatively sta-

tionary patch distribution (Gautestad & Mysterud 2006). While an alternative model area restricted reach (a variant of RW) will lead to longer residence time in high-quality patches; that is, a kind of short-term (tactical) site preference without long-term memory dependence, this behaviour does not implement strategic site fidelity in the sense of MRW. The latter implies a capacity for memory-dependent returns to successful foraging localities ('targets') outside the animal's present perceptual field. Where resources are locally unpredictable but relatively abundant, one may find a switch from LW towards classic RW or correlated RW, as predicted by the Lévy flight foraging hypothesis (Viswanathan *et al.* 1999; Humphries *et al.* 2010, 2012; Sims *et al.* 2012). For example, Sims *et al.* (2012) showed that Brownian motion simulations were not able to reproduce the high-foraging success rate of plankton-feeding basking shark *Cetorhinus maximus* in a heterogeneous resource environment and proposed that a Lévy-like search algorithm may be involved in this species. A memory influence was also proposed, but in a sense of refinement of the search algorithm without explicit consideration of spatial memory (memory map) behind successful patch selection. Simulation of MRW under resource constraint in a Malthusian sense (high-resource density, combined with high local utilization rate) shows a transition towards a nonfractal kind of space use owing to avoidance of – rather than attraction towards – recently visited localities (Gautestad & Mysterud 2010b).

SCALE OF PERCEPTION – EVIDENCE FOR HIERARCHICAL SPACE USE

The three protocols for comparing space use patterns led to similar magnitudes of D when averaging over all series of fixes from red deer, varying in the range $1{\cdot}03 < D < 1{\cdot}25$ (Fig. 4). The result is well below the expectations of $1{\cdot}5 \leq D \ll 2$ from MemRW and correlated RW. MRW can be set to approach a MemRW pattern by changing the Lagrangian parameter $D_{\text{step}} = 1$ for ideal (default) MRW towards $D_{\text{step}} = 2$. This makes the fix pattern more 'space-filling' and RW-like when ignoring the site fidelity aspect, with $D \approx 1{\cdot}4$ (Appendix C, Fig. C1a). The estimated D for red deer is only slightly above the expectation $D \approx 1{\cdot}0$ from simulations of MRW, whereby individuals in the long run put equal weight to choices over a range of scales. For a process characterized by a larger D, more emphasis is put on finer-scale movements on expense of larger-scale moves.

The memory component in MemRW allows for a potential for strategic displacements, that is, space use may be optimized over a large-scale range relative to RW. Still, due to the Markovian structure, reaching long-distance targets (Fig. 1c) will normally become very improbable even with MemRW (see detailed description in Methods). The MemRW design of space use models is a big leap away from classical RW, by explicitly implementing memory in the form of a vector field for bias (Van Moorter *et al.* 2009). However, the actual scale range for space use optimization is susceptible to the strength of this field relative to the other vector components (other fields) representing environmental input.

With respect to Fig. 1d, the bias field constraint was loosened under a postulate of parallel rather than Markovian processing, based on hierarchy theory for complex systems (Allen & Starr 1982, O'Neill *et al.* 1986). The parallel processing postulate for MRW implies that a strategic move is executed at a coarser time and space frame than tactical steps. This allows for many tactical steps to take place while the strategic move is still in progress, but the finer-scaled steps are limited in scope. Both LW and MRW processes may generate a fractal pattern in space ($D \approx 1$) and a power law distribution of step lengths ($\beta \approx 2$), but only MRW involve directed steps towards a target and resilience against frequent directional interrupts from the environment during movement. LW implies serial (Markovian) processing at fine-grained mechanistic scales, while MRW implies parallel processing involving a range of scales.

Since the presence of site fidelity in red deer places MRW rather than LW as a candidate model for deer space use, our analyses open for the inference that red deer in a cognitive manner are expressing parallel processing of scales. Parallel processing of scales can be seen as a difference between more long-distance 'strategic' movements as a contrast to more immediate tactical movements. Indeed, the concept of a hierarchical way of thinking about scaling of space use is taken for granted in the last decades for empirical researchers working with large herbivores (Senft *et al.* 1987; Bailey *et al.* 1996). Senft *et al.* (1987) suggested that habitat selection by herbivores is based on optimizing between maximal quality and adequate quantity over a range of spatial scales. The decisions involve what plants and plant parts to ingest at the finest scales (diet choice), where to graze locally (patch choice), between plant communities at intermediate scales, and landscape features on even larger scales [see also Johnson (1980)]. For red deer in the current case, hierarchical space use may arise at least partly due to movements between day and night habitats (Godvik *et al.* 2009). A future challenge will be to analyse data also at the annual scale, where long-distance seasonally migratory movements of up to more than 50 km may happen (Mysterud *et al.* 2011).The present RW/LW/MemRW/MRW framework (Fig. 1b) brings this conceptual description into the realm of statistical mechanics and provides a theoretical guideline for simulation models at this level. The MRW can be considered the statistical mechanical complement of the more conceptual landscape ecological description of hierarchical scaling.

Conclusion

Our study highlights how simulation models can be used to infer behavioural mechanisms underlying pattern of

space use from GPS data of animal movement. We argue that further progress can be made if the path study model tradition under the Markovian framework (e.g. the RW vs. LW controversy) can implement site fidelity effects – and thus movement rules involving elements of both tactical and strategic displacements – as a consequence of long-term memory. Further, we propose that the home range model tradition should consider more explicitly the premises leading to site fidelity. Finally, we argue that the statistical mechanical approach may lead to a better theoretical coherence between the two traditions. For example, different classes of movement are expected to emerge under different ecological conditions and ultimately contribute to understanding the variable capacity for space use scaling and memory utilization over the animal kingdom.

Acknowledgements

We thank Bram Van Moorter and one anonymous referee for valuable comments. The present manuscript, simulations and data analyses were supported by the AREAL project, funded by the Research Council of Norway ('Natur og Næring'-program; project no. 179370/I10) and the Directorate for Nature Management.

References

Abrahamsen, J., Jacobsen, N.K., Kalliola, R., Dahl, E., Wilborg, L. & Påhlsson, L. (1977) Naturgeografisk regioninndeling av Norden. *Nordiske Utredninger, Series B*, **34**, 1–135.

Allen, T.H.F. & Starr, T.B. (1982) *Hierarchy: perspectives for ecological complexity*. The University of Chicago Press, Chicago

Bailey, D.W. (1995) Daily selection of feeding areas by cattle in homogeneous and heterogeneous environments. *Applied Animal Behaviour Science*, **45**, 183–199.

Bailey, D.W., Gross, J.E., Laca, E.A., Rittenhouse, L.R., Coughenour, M.B., Swift, D.M. & Sims, P.L. (1996) Mechanisms that result in large herbivore grazing distribution patterns. *Journal of Range Management*, **49**, 386–400.

Bartumeus, F. & Levin, S.A. (2008) Fractal reorientation clocks: linking animal behavior to statistical patterns of search. *Proceedings of the National Academy of Sciences of the United States of America*, **105**, 19072–19077.

Börger, L., Dalziel, B.D. & Fryxell, J.M. (2008) Are there general mechanisms of animal home range behaviour? A review and prospects for future research. *Ecology Letters*, **11**, 347–650.

Bouchaud, J.-P. & Georges, A. (1990) Anomalous diffusion in disordered media. Statistical mechanisms, models and physical applications. *Physics reports*, **195**, 127–293.

Burnham, K.P. & Anderson, D.R. (2002) *Model Selection and Multimodel Inference. A Practical Information-Theoretic Approach*. Springer Verlag, New York.

Carranza, J., Alvarez, F. & Redondo, T. (1990) Territoriality as a mating strategy in red deer. *Animal Behaviour*, **40**, 79–88.

Carranza, J., Garcia-Munoz, A.J. & de Dios Vargas, J. (1995) Experimental shifting from harem defence to territoriality in rutting red deer. *Animal Behaviour*, **49**, 551–554.

Clutton-Brock, T.H., Albon, S.D. & Guinness, F.E. (1982) Competition between female relatives in a matrilocal mammal. *Nature*, **300**, 178–180.

Comer, C.E., Kilgo, J.C., D'Angelo, G.J., Glenn, T.C. & Miller, K.V. (2005) Fine-scale genetic structure and social organization in female white-tailed deer. *Journal of Wildlife Management*, **69**, 332–344.

Coulson, T.N., Albon, S.D., Guinness, F.E., Pemberton, J.M. & Clutton-Brock, T.H. (1997) Population substructure, local density, and calf winter survival in red deer (*Cervus elaphus*). *Ecology*, **78**, 852–863.

Dalziel, B.D., Morales, J.M. & Fryxell, J.M. (2008) Fitting probability distributions to animal movement trajectories: using artificial neural networks to link distance, resources and memory. *The American Naturalist*, **172**, 248–258.

Edwards, A.M. (2008) Using likelihood to test for Lévy flight search patterns and for general power-law distributions in nature. *Journal of Animal Ecology*, **77**, 1212–1222.

Edwards, A.M., Phillips, R.A., Watkins, N.W., Freeman, M.P., Murphy, E.J., Afanasyev, V., Buldyrev, S.V., da Luz, M.G.E., Raposo, E.P., Stanley, H.E. & Viswanathan, G.M. (2007) Revisiting Lévy flight search patterns of wandering albatrosses, bumblebees and deer. *Nature*, **449**, 1044–1049.

Feder, J. (1988) *Fractals*. Plenum Press, New York.

Fortin, D., Beyer, H.L., Boyce, M.S., Smith, D.W., Duchesne, T. & Mao, J.S. (2005) Wolves influence elk movements: behavior shapes a tropical cascade in Yellowstone national park. *Ecology*, **86**, 1320–1330.

Gautestad, A.O. (2011) Memory matters: influence from a cognitive map on animal space use. *Journal of Theoretical Biology*, **287**, 26–36.

Gautestad, A.O. (2012) Brownian motion or Lévy walk? Stepping towards an extended statistical mechanics for animal locomotion. *Journal of the Royal Society Interface*, **9**, 2332–2340.

Gautestad, A.O. & Mysterud, I. (2005) Intrinsic scaling complexity in animal dispersion and abundance. *The American Naturalist*, **165**, 44–55.

Gautestad, A.O. & Mysterud, I. (2006) Complex animal distribution and abundance from memory-dependent kinetics. *Ecological Complexity*, **3**, 44–55.

Gautestad, A.O. & Mysterud, I. (2010a) The home range fractal: from random walk to memory dependent space use. *Ecological Complexity*, **7**, 458–470.

Gautestad, A.O. & Mysterud, I. (2010b) Spatial memory, habitat autofacilitation and the emergence of fractal home range patterns. *Ecological Modelling*, **221**, 2741–2750.

Gautestad, A. & Mysterud, I. (2012) The dilution effect and the space fill effect: seeking to offset statistical artifacts when analyzing animal space use from telemetry fixes. *Ecological Complexity*, **9**, 33–42.

Georgii, B. (1981) Activity patterns of female red deer (*Cervus elaphus* L.) in the Alps. *Oecologia*, **49**, 127–136.

Getz, W.M. & Saltz, D. (2008) A framework for generating and analyzing movement paths on ecological landscapes. *Proceedings of the National Academy of Sciences of the United States of America*, **105**, 19066–19071.

Godvik, I.M.R., Loe, L.E., Vik, J.O., Veiberg, V., Langvatn, R. & Mysterud, A. (2009) Temporal scales, trade-offs and functional responses in habitat selection of red deer. *Ecology*, **90**, 699–710.

Hafting, T., Fyhn, M., Molden, S., Moser, M.-B. & Moser, E.I. (2005) Microstructure of a spatial map in the entorhinal cortex. *Nature*, **436**, 801–806.

Hagen, C.A., Kenkel, N.C., Walker, D.J., Baydack, R.K. & Braun, C.E. (2001) Fractal-based spatial analysis of radiotelemetry data. *Radio Tracking and Animal Populations* (eds J.J. Millspaugh & J.M. Marzluff), pp. 167–187. Academic Press, San Diego.

Hays, G.C., Bastian, T., Doyle, T.K., Fossette, S., Gleiss, A.C., Gravenor, M.B., Hobson, V.J., Humphries, N.E., Lilley, M.K.S., Pade, N.G. & Sims, D.W. (2012) High activity and Lévy searches: jellyfish can search the water column like a fish. *Proceedings of the Royal Society B*, **279**, 465–473.

Humphries, N.E., Queiroz, N., Dyer, J.R.M., Pade, N.G., Musyl, M.K., Schaefer, K.M., Fuller, D.W., Brunnschweiler, J.M., Doyle, T.K., Houghton, J.D.R., Hays, G.C., Jones, C.S., Noble, L.R., Wearmouth, V.J., Southhall, E.J. & Sims, D.W. (2010) Environmental context explains Lévy and Brownian movement patterns of marine predators. *Nature*, **465**, 1066–1069.

Humphries, N.E., Weimerskirch, H., Queiroz, N., Southhall, E.J. & Sims, D.W. (2012) Foraging success of biological Lévy flights recorded in situ. *Proceedings of the National Academy of Sciences of the United States of America*, **109**, 7169–7174.

Jędrzejewski, W., Schmidt, K., Theuerkauf, J., Jędrzejewska, B. & Kowalczyk, R. (2007) Territory size of wolves Canis lupus: linking local (Biaowieża Primeval Forest, Poland) and Holarctic-scale patterns. *Ecography*, **30**, 66–76.

Johnson, D.H. (1980) The comparison of usage and availability measurements for evaluating resource preference. *Ecology*, **61**, 65–71.

Langvatn, R., Mysterud, A., Stenseth, N.C. & Yoccoz, N.G. (2004) Timing and synchrony of ovulation in red deer constrained by short northern summers. *The American Naturalist*, **163**, 763–772.

Loe, L.E., Bonenfant, C., Mysterud, A., Gaillard, J.-M., Langvatn, R., Stenseth, N.C., Klein, F., Calenge, C., Ergon, T. & Pettorelli, N. (2005) Climate predictability and breeding phenology in red deer: timing and

synchrony of rutting and calving in Norway and France. *Journal of Animal Ecology*, **74**, 579–588.
Mandelbrot, B.B. (1983) *The Fractal Geometry of Nature*. W. H. Freeman and Company, New York.
Morales, J.M., Haydon, D.T., Frair, J., Holsinger, K.E. & Fryxell, J.M. (2004) Extracting more out of relocation data: building movement models as mixtures of random walks. *Ecology*, **85**, 2436–2445.
Mueller, T. & Fagan, W.F. (2008) Search and navigation in dynamic environments - from individual behaviors to population distributions. *Oikos*, **117**, 654–664.
Mueller, T., Fagan, W.F. & Grimm, V. (2011) Integrating individual search and navigation behaviors in mechanistic movement models. *Theoretical Ecology*, **4**, 341–355.
Muggeo, V.M.R. (2008) Segmented: an R package to fit regression models with broken-line relationships. *R News*, **8**, 20–25.
Mysterud, A., Langvatn, R., Yoccoz, N.G. & Stenseth, N.C. (2002) Large-scale habitat variability, delayed density effects and red deer populations in Norway. *Journal of Animal Ecology*, **71**, 569–580.
Mysterud, A., Loe, L.E., Zimmermann, B., Bischof, R., Veiberg, V. & Meisingset, E.L. (2011) Partial migration in expanding red deer populations at northern latitudes – a role for density dependence? *Oikos*, **120**, 1817–1825.
Nathan, R., Getz, W.M., Revilla, E., Holyoak, M., Kadmon, R., Saltz, D. & Smouse, P.E. (2008) A movement ecology paradigm for unifying organismal movement research. *Proceedings of the National Academy of Sciences of the United States of America*, **105**, 19052–19059.
O'Neill, R.V., DeAngelis, D.L., Wade, J.B. & Allen, T.F.H. (1986) A Hierarchical Concept of Ecosystems. *Monographs in Population Biology*, pp. 253. Princeton University Press, Princeton.
Ostfeld, R.S. & Manson, R.H. (1996) Long-distance homing in meadow voles, *Microtus pennsylvanicus*. *Journal of Mammalogy*, **77**, 870–873.
Piper, W.H. (2011) Making habitat selection more "familiar": a review. *Behavioral Ecology and Sociobiology*, **65**, 1329–1351.
Reynolds, A.M. (2010) Animals that randomly reorient at cues left by correlated random walkers do the Lévy walk. *The American Naturalist*, **175**, 607–613.
Rhim, S.J. & Lee, W.S. (2004) Seasonal changes in territorial behaviour of hazel grouse (Bonasa bonasia) in a temperate forest of South Korea. *Journal of Ornithology*, **145**, 31–34.
Rivrud, I.M., Loe, L.E. & Mysterud, A. (2010) How does local weather predict red deer home range size at different temporal scales? *Journal of Animal Ecology*, **79**, 1280–1295.
Senft, R.L., Coughenour, M.B., Bailey, D.W., Rittenhouse, L.R., Sala, O.E. & Swift, D.M. (1987) Large herbivore foraging and ecological hierarchies. *BioScience*, **37**, 789–799.
Sims, D.W., Witt, M.J., Richardson, A.J., Southhall, E.J. & Metcalfe, J.D. (2006) Encounter success of free-ranging marine predator movements across a dynamic prey landscape. *Proceedings of the Royal Society B*, **273**, 1195–1201.
Sims, D.W., Southall, E.J., Humphries, N.E., Hays, G.C., Bradshaw, C.J.A., Pitchford, J.W., James, A., Ahmed, M.Z., Brierley, A.S., Hindell, M.A., Morritt, D., Musyl, M.K., Righton, D., Shepard, E.L.C., Wearmouth, V.J., Wilson, R.P., Witt, M.J. & Metcalfe, J.D. (2008) Scaling laws of marine predator search behaviour. *Nature*, **451**, 1098–1103.
Sims, D.W., Humphries, N.E., Bradford, R.W. & Bruce, B.D. (2012) Lévy flight and Brownian search patterns of a free-ranging predator reflect different prey field characteristics. *Journal of Animal Ecology*, **81**, 432–442.
Sugihara, G. & May, R.M. (1990) Applications of fractals in ecology. *Trends in Ecology & Evolution*, **5**, 79–86.
Swihart, R.K. & Slade, N.A. (1985) Influence of sampling interval on estimates of home-range size. *Journal of Range Management*, **49**, 1019–1025.
Turchin, P. (1996) Fractal analyses of animal movement: a critique. *Ecology*, **77**, 2086–2090.
Van Moorter, B., Visscher, D., Benhamou, S., Börger, L., Boyce, M.S. & Gaillard, J.-M. (2009) Memory keeps you at home: a mechanistic model for home range emergence. *Oikos*, **118**, 641–652.
Van Moorter, B., Visscher, D., Herfindal, I., Basille, M. & Mysterud, A. (2012) Inferring behavioral mechanisms in habitat selection studies – getting the null-hypothesis right for functional and familiarity responses. *Ecography*, doi: 10.1111/j.1600-0587.2012.07291.x.
Viswanathan, G.M., Buldyrev, S.V., Havlin, S., daLuz, M.G.E., Raposo, E.P. & Stanley, H.E. (1999) Optimizing the success of random searches. *Nature*, **401**, 911–914.
Viswanathan, G.M., Afanasyev, V., Buldyrev, S.V., Havlin, S., da Luz, M.G.E., Raposo, E.P. & Stanley, H.E. (2000) Lévy flights in random searches. *Physica A*, **282**, 1–12.
Viswanathan, G.M., da Luz, M.G.E., Raposo, E.P. & Stanley, H.E. (2011) *The Physics of Foraging: An Introduction to Random Searches and Biological Encounters*. Cambridge University Press, Cambridge.
Wolf, M., Frair, J.L., Merrill, E. & Turchin, P. (2009) The attraction of the known: the importance of spatial familiarity in habitat selection in wapiti *Cervus elaphus*. *Ecography*, **32**, 401–410.
Wood, S. (2006) *Generalized Additive Models: An Introduction with R*. Chapman & Hall/CRC, Boca Raton, FL.
Zuur, A.F., Leno, E.N., Walker, N., Saveliev, A.A. & Smith, G.M. (2009) *Mixed Effects Models and Extensions in Ecology with R*. Springer, Berlin.

Received 21 March 2012; accepted 19 October 2012
Handling Editor: Tim Coulson

Supporting Information

Additional Supporting Information may be found in the online version of this article.

Appendix S1. Model concepts related to memory and scaling.

Appendix S2. Fractal analysis of MRW simulations.

Appendix S3. Fractal analysis of MemRW simulations.

Appendix S4. Estimating slope Z under Protocol 3.

Appendix S5. Detailed statistical analyses of Individual red deer time series.